Inorg. Chem. **2006**, *45*, 6014–6019

Inorganic Chemistry
Article

Molecular Structures of *arachno*-Decaborane Derivatives 6,9-$X_2B_8H_{10}$ (X = CH_2, NH, Se) Including a Gas-Phase Electron-Diffraction Study of 6,9-$C_2B_8H_{14}$

Drahomír Hnyk,[†] Michael Bühl,[§] Josef Holub,[†] Stuart A. Hayes,[‡] Derek A. Wann,[‡] Iain D. Mackie,[‡] Konstantin B. Borisenko,[‡] Heather E. Robertson,[‡] and David W. H. Rankin*[,‡]

Institute of Inorganic Chemistry, Academy of Sciences of the Czech Republic,
25068 Řež, Czech Republic, Max-Planck-Institut für Kohlenforschung, Kaiser-Wilhelm-Platz 1,
45470 Mülheim an der Ruhr, Germany, and School of Chemistry, University of Edinburgh,
West Mains Road, Edinburgh, EH9 3JJ, United Kingdom

Received February 21, 2006

The molecular structures of the three heterodecaboranes *arachno*-6,9-$C_2B_8H_{14}$, *arachno*-6,9-$N_2B_8H_{12}$, and *arachno*-6,9-$Se_2B_8H_{10}$ have been determined by ab initio MO theory. In addition, the structure of *arachno*-6,9-$C_2B_8H_{14}$ was experimentally determined using gas-phase electron diffraction (GED). The accuracy of all four of these structures has been confirmed by the good agreement of the ^{11}B chemical shifts calculated at the GIAO-MP2 level with the experimental values. A comparison of the GIAO-HF and GIAO-MP2 methods shows that for these heteroborane clusters, electron correlation effects on the computed $\delta(^{11}B)$ values are quite substantial and that it is necessary to go beyond the HF level in the NMR computation.

Introduction

The boranes and heteroboranes of the arachno 10-vertex series are an important class of compounds in boron chemistry because of the roles they play in systematic building and degradation processes, leading to clusters of larger and smaller dimensions, respectively.[1] This family of compounds is based on the parent $[arachno\text{-}B_{10}H_{14}]^{2-}$ (Figure 1, **1**),[2] from which the family members are formally derived by replacing the $\{BH_2\}^-$ cluster vertices with units that are isoelectrolobal[3] with $\{BH_2\}^-$, for example, $\{CH_2\}$, $\{NH\}$, or $\{S\}$. According to Gimarc's topological rule,[4] elements more electronegative than boron (C, N, S) prefer cluster sites of the highest electron density. According to natural population analysis (NPA), these sites in **1** correspond to positions 6 and 9.[5] Indeed, various synthetic routes lead both to anionic monoheteroatomic species such as $[6\text{-}CB_9H_{14}]^-$,[6] $[6\text{-}NB_9H_{13}]^-$,[7] and $[6\text{-}SB_9H_{12}]^-$,[8] and neutral species represented by dihet-

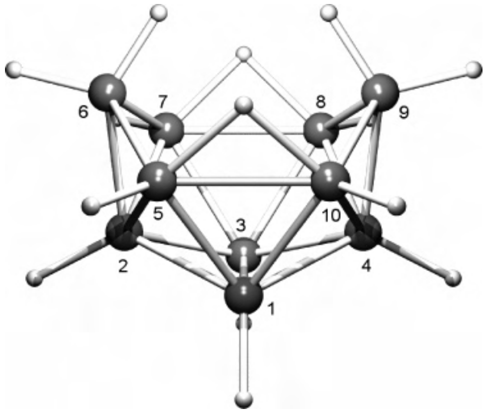

Figure 1. Molecular structure of $[arachno\text{-}B_{10}H_{14}]^{2-}$, **1**, showing boron numbering.

---

* To whom correspondence should be addressed. E-mail: dwhrankin@ed.ac.uk.

[†] Academy of Sciences of the Czech Republic.

[§] Max-Planck-Institut für Kohlenforschung.

[‡] University of Edinburgh.

(1) (a) Štíbr, B.; Plešek, J.; Heřmánek, S. In *Advances in Boron and the Boranes*; Liebman, J. F., Williams, R. E., Eds.; VCH Publishers: New York, 1988; p 35. (b) Štíbr, B.; Plešek, J.; Jelínek, T.; Baše, K.; Janoušek, Z.; Heřmánek, S. In *Boron Chemistry*; Heřmánek, S., Ed.; World Scientific: Singapore, 1988; p 175.

(2) Kendall, D. S.; Lipscomb, W. N. *Inorg. Chem.* **1973**, *12*, 546 and references therein.

(3) For a definition of isoelectrolobal, see, for example: Beckett, M. A.; Crook, J. E.; Greenwood, N. N.; Kennedy, J. D. *J. Chem. Soc., Dalton Trans.* **1986**, 1879.

(4) Ott, J. J.; Gimarc, B. M. *J. Am. Chem. Soc.* **1986**, *108*, 4303.

(5) Hnyk, D.; Holub, J. *Collect. Czech. Chem. Commun.* **2002**, *67*, 813. Note that another popular population analysis based on the Mulliken scheme affords a different result; the drawbacks of the Mulliken approach are well-known. See, for example: Reed, A. E.; Weinstock, R. B.; Weinhold, F. *J. Chem. Phys.* **1985**, *83*, 735.

10.1021/ic060296v CCC: $33.50

eroatomic compounds 6,9-$C_2B_8H_{14}$,[9] 6,9-$N_2B_8H_{12}$,[10] and even 6,9-$Se_2B_8H_{10}$.[11]

Very little is known about the structures of such compounds formally derived from **1**. Single crystals cannot normally be grown, precluding the use of X-ray crystallography to determine their molecular structures in the solid state. On the other hand, structural assignments determined on the basis of the ab initio/IGLO (or more recently GIAO)/NMR method[12] are quickly approaching a confidence level that rivals modern-day X-ray determinations of molecular structures.[13] Theoretical assessments of structures are made not only on the basis of computed geometries but also on chemical shift calculations (IGLO or GIAO), because $\delta(^{11}B)$ values are very sensitive to small geometric changes. The level of agreement between calculated and experimental ^{11}B chemical shifts serves as a criterion for assessing the accuracy of a particular geometry. This approach derives the molecular structures of molecules under the conditions of the NMR experiments, i.e., in dilute solutions. Free neutral heteroboranes have also been investigated in the gas phase by electron diffraction, with a lot of work performed on carbaboranes;[14] azaboranes and thiaboranes have been investigated to a lesser extent.[15,12d] To gain a deeper insight into the molecular structures of carbaboranes, azaboranes and, for the first time, selenaboranes, in conjunction with 10-vertex arachno species, we have undertaken a structural study of the experimentally available compounds **2**−**4** (Figures 2−4, respectively) using the ab initio/GIAO/NMR method. The structure of **2** was determined using the combination of this structural tool together with gas-phase electron diffraction (GED).

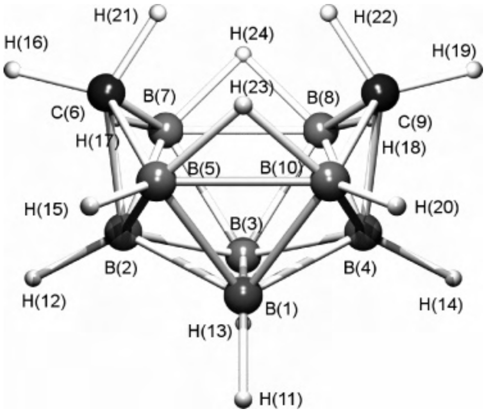

Figure 2. Molecular structure of *arachno*-6,9-$C_2B_8H_{14}$, **2**, showing atom numbering.

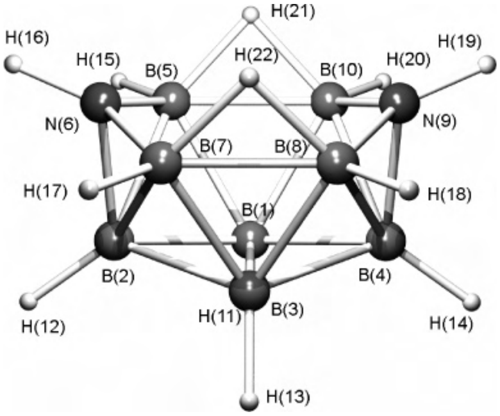

Figure 3. Molecular structure of *arachno*-6,9-$N_2B_8H_{12}$, **3**, showing atom numbering.

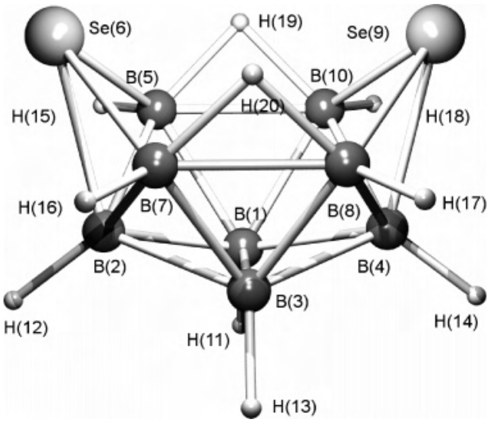

Figure 4. Molecular structure of *arachno*-6,9-$Se_2B_8H_{10}$, **4**, showing atom numbering.

---

(6) Fontaine, X. L. R.; Kennedy, J. D.; Thornton-Pett, M.; Nestor, K.; Štíbr, B.; Jelínek, T.; Baše, K. *J. Chem. Soc., Dalton Trans.* **1990**, 2887.

(7) (a) Hertler, W. R.; Klanberg, F.; Muetterties, E. L. *Inorg. Chem.* **1967**, *6*, 1696.(b) Baše, K.; Hanousek, F.; Štíbr, B.; Plešek, J.; Lyèka, J. *J. Chem. Soc., Chem. Commun.* **1981**, 1163. (c) Baše, K. *Collect. Czech. Chem. Commun.* **1983**, *48*, 2593.

(8) (a) Rudolph, R. W.; Pretzer, R. W. *Inorg. Synth.* **1983**, *22*, 226. (b) Siedle, A. R.; Bodner, G. M.; Garber, A. R.; McDowell, D.; Todd, L. J. *Inorg. Chem.* **1974**, *13*, 1756. (c) Bown, M.; Fontaine, X. L. R.; Kennedy, J. D. *J. Chem. Soc., Dalton Trans.* **1988**, 1467.

(9) Štíbr, B.; Plešek, J.; Heømánek, S. *Collect. Czech. Chem. Commun.* **1974**, *39*, 1805.

(10) Štíbr, B.; Kennedy, J. D.; Jelínek, T. *J. Chem. Soc., Chem. Commun.* **1990**, 1309.

(11) Friesen, G. D.; Barriola, A.; Todd, L. J. *Chem. Ind.* **1978**, 631.

(12) (a) Bühl, M.; Schleyer, P. v. R. *J. Am. Chem. Soc.* **1992**, *114*, 477. Some other examples of the ab initio/IGLO/NMR approach include: (b) A C_1 form of B_5H_{11} is favored over the C_s structure; Schleyer, P. v. R.; Bühl, M.; Fleischer, U.; Koch, W. *Inorg. Chem.* **1990**, *29*, 153. (c) The structure of *nido*-$C_2B_6H_{10}$; Bausch, J. W.; Prakash, G. K. S.; Bühl, M.; Schleyer, P. v. R.; Williams, R. E. *Inorg. Chem.* **1992**, *31*, 3060. (d) A theoretical and experimental refinement of *closo*-1-$NB_{11}H_{12}$; Hnyk, D.; Bühl, M.; Schleyer, P. v. R.; Volden, H. V.; Gundersen, S.; Müller, J.; Paetzold, P. *Inorg. Chem.* **1993**, *32*, 2442. For further references see: (e) Bühl, M., Schleyer, P. v. R. In *Electron Deficient Boron and Carbon Clusters*; Olah, G. A., Wade, K., Williams, R. E., Eds.; Wiley: New York, 1991; p 113. (f) Diaz, M.; Jaballas, T.; Arias, J.; Lee, H.; Onak, T. *J. Am. Chem. Soc.* **1996**, *118*, 4405 and references therein. (g) Bühl, M. NMR Chemical Shift Computation: Structural Applications. In *Encyclopedia of Computational Chemistry*; Schleyer, P. v. R., Allinger, N. L., Clark, T., Gasteiger, J., Kollman, P. A., Schaefer, H. F., Schreiner, P. R., Eds.; John Wiley and Sons: Chichester, U.K., 1998; Vol. 3, p 1835. The most recent applications of ab initio/GIAO/NMR: (h) Holub, J.; Jelínek, T.; Hnyk, D.; Plzák, Z.; Císaøová, I.; Bakardjiev, M.; Štíbr, B. *Chem.*−*Eur. J.* **2001**, *7*, 1546. (i) Štíbr, B.; Tok, O. L.; Milius, W.; Bakardjiev, M.; Holub, J.; Hnyk, D.; Wrackmeyer, B. *Angew. Chem., Int. Ed.* **2002**, *41*, 2126.

(13) Onak, T.; Tseng, J.; Diaz, M.; Tran, D.; Arias, J.; Herrera, S.; Brown, D. *Inorg. Chem.* **1993**, *32*, 487.

(14) (a) Turner, A. R.; Robertson, H. E.; Borisenko, K. B.; Rankin, D. W. H.; Fox, M. A. *Dalton Trans.* **2005**, 1310. (b) Mackie, I. D.; Robertson, H. E.; Rankin, D. W. H.; Fox, M. A.; Malget, J. M. *Inorg. Chem.* **2004**, *43*, 5387. (c) Fox, M. A.; Greatrex, R.; Nikrahi, A.; Brain, P. T.; Picton, M. J.; Rankin, D. W. H.; Robertson, H. E.; Bühl, M.; Li, L.; Beaudet, R. A. *Inorg. Chem.* **1998**, *37*, 2166. (d) Hynk, D.; Hofmann, M.; Schleyer, P. v. R.; Bühl, M.; Rankin, D. W. H. *J. Phys. Chem.* **1996**, *100*, 3435. (e) Hynk, D.; Rankin, D. W. H.; Robertson, H. E.; Hofmann, M.; Schleyer, P. v. R.; Bühl, M. *Inorg. Chem.* **1994**, *33*, 4781. (f) Hosmane, N. S.; Maldar; N. N.; Potts, S. B.; Rankin, D. W. H.; Robertson, H. E. *Inorg. Chem.* **1986**, *25*, 1561.

Experimental Section

Computational Details. The geometries of compounds **2**−**4** were fully optimized in C_{2v} symmetry using the Gaussian 03 suite of programs,[16] first at a RHF level with the standard 6-31G* basis set[17] for C, N, B, and H and with the all-electron basis sets 641(d) and 962(d)[18] for Se. The character of each stationary point for each system was verified by frequency calculations followed by further optimizations at the correlated MP2/6-31G* (for **2** and **3**) and MP2/962(d) (for **4**) levels.[19] For comparison with the all-electron calculations, *arachno*-$Se_2B_8H_{10}$ was also optimized using a quasirelativistic, Stuttgart−Dresden effective-core potential ECP[20] for Se with a polarized double-ζ valence basis set augmented with a diffuse sp set[21] and a d-polarization function[22] [ECP+(d) notation].

Magnetic shieldings were calculated using the GIAO-HF and GIAO-MP2 methods,[23] incorporated into Gaussian 03 utilizing the IGLO-II basis[24] for C, B, N, and H and three different basis sets for Se: 962+(d),[25] ECP+(d) (see above), and IGLO-II without f functions.[26] Additional NMR calculations were performed for the RMP2/962(d)-optimized geometry of *arachno*-$Se_2B_8H_{10}$ with the Amsterdam density functional (ADF) code[27,28] employing the BP86 functional.[29] The two-component relativistic zeroth-order regular approximation (ZORA) method,[30] including scalar and spin−orbit (SO)[31] corrections, has been employed for the computations. We have used the triple-ζ basis set plus one polarization function (denoted TZP) from the ADF library for all atoms. ^{11}B chemical shifts were calculated relative to B_2H_6, with an absolute shielding of 120.0, 96.9, and 79.1 ppm at the GIAO-HF/II, GIAO-MP2/II, and ZORA-SO/BP86/TPZ levels, respectively (all employing the MP2/6-31G* geometry), and converted to the usual $BF_3 \cdot OEt_2$ scale using the experimental $\delta(^{11}B)$ value of B_2H_6, 16.6 ppm.[13] The NMR results are given in Table 1.[32]

Table 1. Calculated and Experimental ^{11}B NMR Chemical Shifts for **2**−**4**[a,b]

	$\delta(^{11}B)$ (ppm)		
	B(1,3)	B(2,4)	B(5,7,8,10)
arachno-6,9-$C_2B_8H_{14}$, **2**			
GIAO-HF/II//RMP2(fc)/6-31G*	−35.5	10.8	−14.1
GIAO-HF/II//GED	−34.5	11.5	−13.1
GIAO-MP2/II//RMP2(fc)/6-31G*	−37.1	5.2	−17.0
GIAO-MP2/II//GED	−36.0	6.0	−15.9
experimental [c]	−37.7	3.7	−17.5
arachno-6,9-$N_2B_8H_{12}$, **3**			
GIAO-HF/II//RMP2(fc)/6-31G*	−40.5	11.7	−21.3
GIAO-MP2/II//RMP2(fc)/6-31G*	−41.7	7.3	−25.8
experimental[d]	−41.0	7.3	−25.7
arachno-6,9-$Se_2B_8H_{10}$, **4**			
GIAO-HF/IGLO-II//RMP2/962(d)[e]	−29.9	21.4	−11.7
GIAO-HF/ECP+DZ+(d)//RMP2/962(d)[e]	−29.5	22.0	−10.9
GIAO-HF/962(+)d//RMP2/962(d)[e]	−29.8	21.4	−11.7
ZORA-DFT/TZP//RMP2/962(d)[f]	−36.1	10.1	−22.7
GIAO-MP2/962(+)d//RMP2/962(d)[e]	−30.2	17.0	−15.5
experimental [g]	−30.7	14.9	−16.9

[a] See Figures 1−3 for atom numbering of **2**−**4**, respectively. [b] Relative to $BF_3 \cdot OEt_2$, see text for description. [c] See ref 9. [d] See ref 10. [e] For notation, see text. [f] SO coupling included, see text for description. [g] See ref 11.

Electron Diffraction

Data were collected using the Edinburgh gas electron-diffraction apparatus,[33] with an accelerating voltage of ca. 40 kV (ca. 6.0 pm electron wavelength) on Kodak Electron Image film. Nozzle-to-camera distances were calculated using benzene vapor as a standard, immediately after recording the diffraction pattern of **2**. Respective sample and nozzle temperatures of 453 and 493 K were used at the short nozzle-to-camera distance (96.0 mm), and those at the

---

(15) (a) Electron-diffraction study of *closo*-1-$SB_{11}H_{11}$: Hnyk, D.; Vajda, E.; Bühl, M.; Schleyer, P. v. R. *Inorg. Chem.* **1992**, *31*, 2464. (b) A theoretical and experimental (GED) refinement of *closo*-1-$NB_{11}H_{12}$: Hnyk, D.; Bühl, M.; Schleyer, P. v. R.; Volden, H. V.; Gundersen, S.; Müller, J.; Paetzold, P. *Inorg. Chem.* **1993**, *32*, 2442.

(16) Frisch, M. J.; Trucks, G. W.; Schlegel, H. B.; Scuseria, G. E.; Robb, M. A.; Cheeseman, J. R.; Montgomery, J. A., Jr.; Vreven, T.; Kudin, K. N.; Burant, J. C.; Millam, J. M.; Iyengar, S. S.; Tomasi, J.; Barone, V.; Mennucci, B.; Cossi, M.; Scalmani, G.; Rega, N.; Petersson, G. A.; Nakatsuji, H.; Hada, M.; Ehara, M.; Toyota, K.; Fukuda, R.; Hasegawa, J.; Ishida, M.; Nakajima, T.; Honda, Y.; Kitao, O.; Nakai, H.; Klene, M.; Li, X.; Knox, J. E.; Hratchian, H. P.; Cross, J. B.; Adamo, C.; Jaramillo, J.; Gomperts, R.; Stratmann, R. E.; Yazyev, O.; Austin, A. J.; Cammi, R.; Pomelli, C.; Ochterski, J. W.; Ayala, P. Y.; Morokuma, K.; Voth, G. A.; Salvador, P.; Dannenberg, J. J.; Zakrzewski, V. G.; Dapprich, S.; Daniels, A. D.; Strain, M. C.; Farkas, O.; Malick, D. K.; Rabuck, A. D.; Raghavachari, K.; Foresman, J. B.; Ortiz, J. V.; Cui, Q.; Baboul, A. G.; Clifford, S.; Cioslowski, J.; Stefanov, B. B.; Liu, G.; Liashenko, A.; Piskorz, P.; Komaromi, I.; Martin, R. L.; Fox, D. J.; Keith, T.; Al-Laham, M. A.; Peng, C. Y.; Nanayakkara, A.; Challacombe, M.; Gill, P. M. W.; Johnson, B.; Chen, W.; Wong, M. W.; Gonzalez, C.; Pople, J. A. *Gaussian 03*, revision B.02; Gaussian, Inc.: Pittsburgh, PA, 2003.

(17) Hehre, W.; Radom, L.; Schleyer, P. v. R.; Pople, J. A. *ab Initio Molecular Orbital Theory*; Wiley: New York, 1986.

(18) Binning and Curtiss' [6s4p1d] contraction (Binning, R. C.; Curtiss, L. A. *J. Comput. Chem.* **1990**, *11*, 1206) of Dunning's (14s11p5d) primitive set (Dunning, T. H. *J. Chem. Phys.* **1977**, *66*, 1382) augmented with one set of d polarization functions ($\alpha_d = 0.315$).

(19) Although experimental attempts to prepare *arachno*-$S_2B_8H_{10}$ failed, we optimized its structure at the RMP2(fc)/6-31G* level. HF/6-31G* showed this system to represent a minimum on its potential-energy hypersurface.

(20) Berger, A.; Dolg, M.; Küchle, W.; Stoll, H.; Preuss, H. *Mol. Phys.* **1993**, *80*, 1431.

(21) El-Nahas, A. E.; Schleyer, P. v. R. *J. Comput. Chem.* **1994**, *15*, 596.

(22) Huzinaga, S., Ed. *Gaussian Basis Sets for Molecular Calculations*; Elsevier: New York, 1984.

(23) (a) Ditchfield, R. *Mol. Phys.* **1974**, *27*, 789. (b) Wolinski, K.; Hinton, J. F.; Pulay, P. *J. Am. Chem. Soc.* **1990**, *112*, 8251. (c) Gauss, J. *J. Chem. Phys.* **1993**, *99*, 3629.

(24) Kutzelnigg, W.; Fleischer, U.; Schindler, M. *NMR Basic Principles and Progress*; Springer: Berlin, 1990; Vol. 23, pp 165−262.

(25) Same as 962(d), augmented with one set of diffuse s and p functions.

(26) (15s11p7d2f) contracted to [10s9p5d], cf. (a) Fleischer, U. Ph.D. Thesis, Ruhr-UniversitätBochum, Bochum, Germany, 1992. (b) Bühl, M.; Thiel, W.; Fleischer, U.; Kutzelnigg, W. *J. Phys. Chem.* **1995**, *99*, 4000, cf. ref 18.

(27) (a) Baerends, E. J.; Ellis, D. E.; Ros, P. *Chem. Phys.* **1973**, *2*, 41. (b) te Velde, G.; Baerends, E. J. *J. Comput. Phys.* **1992**, *99*, 84. (c) Fonseca Guerra, C.; Snijders, J. G.; te Velde, G.; Baerends, E. J. *Theor. Chem. Acta* **1998**, *99*, 391. (d) te Velde, G.; Bickelhaupt, F. M.; Baerends, E. J.; Fonseca Guerra, C.; van Gisbergen, S. J. A.; Snijders, J. G.; Ziegler, T. *J. Comput. Chem.* **2001**, *22*, 931.

(28) Baerends, E. J.; Autschbach, J.; Bérces, A.; Bo, C.; Boerrigter, P. M.; Cavallo, L.; Chong, D. P.; Deng, L.; Dickson, R. M.; Ellis, D. E.; Fan, L.; Fischer, T. H.; Fonseca Guerra, C.; van Gisbergen, S. J. A.; Groeneveld, J. A.; Gritsenko, O. V.; Grüning, M.; Harris, F. E.; van den Hoek, P.; Jacobsen, H.; van Kessel, G.; Kootstra, F.; van Lenthe, E.; McCormack, D. A.; Osinga, V. P.; Patchkovskii, S.; Philipsen, P. H. T.; Post, D.; Pye, C. C.; Ravenek, W.; Ros, P.; Schipper, P. R. T.; Schreckenbach, G.; Snijders, J. G.; Sola, M.; Swart, M.; Swerhone, D.; te Velde, G.; Vernooijs, P.; Versluis, L.; Visser, O.; van Wezenbeek, E.; Wiesenekker, G.; Wolff, S. K.; Woo, T. K.; Ziegler, T. *ADF2004.01*; SCM, Theoretical Chemistry, Vrije Universiteit: Amsterdam, The Netherlands, 2004.

(29) (a) Becke, A. D. *Phys. Rev. A* **1988**, *38*, 3098. (b) Perdew, J. P. *Phys. Rev. B* **1986**, *33*, 8822.

(30) (a) van Lenthe, E.; Baerends, E. J.; Snijders, J. G. *J. Chem. Phys.* **1994**, *101*, 9783. (b) van Lenthe, E.; van Leeuwen, R.; Baerends, E. J.; Snijders, J. G. *Int. J. Quantum Chem.* **1996**, *57*, 281. (c) van Lenthe, E., Baerends, E. J.; Snijders, J. G. *J. Chem. Phys.* **1993**, *99*, 4597.

(31) van Lenthe, E.; Snijders, J. G.; Baerends, E. J. *J. Chem. Phys.* **1996**, *105*, 6505.

(32) The GIAO-HF/II//RMP2(fc)/6-31G* results for *arachno*-$S_2B_8H_{10}$ are (in ppm): B(1, 3) = −32.9; B(2, 4) = 18.4; B(5, 7, 8, 10) = −16.0.

(33) Huntley, C. M.; Laurenson, G. S.; Rankin, D. W. H. *J. Chem. Soc., Dalton Trans.* **1980**, 954.

Table 2. Experimental and Theoretical Geometric Parameters for **2**^{a}

	description	value	restraint^b	MP2/6-31G*
independent parameters				
p_1	*r*B−B average	179.1(2)		178.0
p_2	*r*B(1)−B(3) − *r*B(1)−B(2)	6.9(4)	7.1(5)	7.1
p_3	*r*B(1)−B(3) − *r*B(1)−B(5)	2.0(5)	1.8(5)	1.8
p_4	∠X−O−B(4) ^{c}	20.2(3)		20.3
p_5	*r*O−C^c	268.4(6)		267.7
p_6	∠X−O−C(9)^c	54.4(2)		54.0
p_7	∠B(5)−B(1)−B(3)	107.7(1)		107.3
p_8	*r*B/C−H average	121.0(4)		119.7
p_9	*r*B/C−H diff 1	22.7(5)	22.7(5)	22.7
p_{10}	*r*B/C−H diff 2	12.7(4)	12.5(5)	12.5
p_{11}	∠B(3)−B(1)−H(11)	120.3(5)	120.3(5)	120.3
p_{12}	∠B(4)−B(2)−H(12)	152.7(5)	152.7(5)	152.7
p_{13}	∠B(1)−B(5)−H(15)	120.0(5)	120.0(5)	120.0
p_{14}	∠B(2)−C(6)−H(16)	109.9(5)	109.8(5)	109.8
p_{15}	∠B(2)−C(6)−H(21)	140.5(5)	140.4(5)	140.4
p_{16}	*φ*B(5)−B(1)−B(3)−B(4)	103.1(4)		102.7
p_{17}	*φ*B(3)−B(1)−B(5)−H(15)	144.4(9)	145.6(10)	145.6
p_{18}	*φ*B(8)−B(10)−B(5)−H(23)	−106.9(5)	−106.5(5)	−106.5
dependent parameters				
d_1	*r*B(5)−C − *r*B(2)−C	8.0(4)	7.7(5)	7.7
d_2	*r*B(5)−B(2) − *r*B(5)−C	3.5(3)	3.2(5)	3.2
d_3	*r*B(1)−B(2) − *r*B(5)−C	0.1(2)	0.2(2)	0.2
d_4	*r*B(5)−B(10) − *r*B(2)−B(5)	9.5(4)	9.6(5)	9.6

^{a} All distances in picometers, angles in degrees. ^{b} Restraint uncertainties derived from the degree of convergence of calculations are shown in parentheses. ^{c} O is the origin and X refers to the positive direction of the *x* axis.

long nozzle-to-camera distance (257.1 mm) were 416 and 458 K. The electron-scattering patterns were converted into digital form using an Epson Expression 1680 Pro flatbed scanner with a scanning program described previously.[34] Data reduction and least-squares refinements were carried out using the ed@ed program,[35] employing the scattering factors of Ross et al.[36] The scale factors, *s* limits, weighting points, correlation parameters, and electron wavelengths are provided in the Supporting Information (Table S1).

A molecular model was written for **2**, converting the refineable independent parameters into atomic Cartesian coordinates. This model was constructed assuming C_{2v} symmetry, as exhibited by the calculated geometries and ^{11}B NMR experimental data, allowing the structure to be defined in terms of 18 independent parameters (p_1−p_{18}, Table 2). Three of these parameters were used to define the lengths of the bonds, namely B(1)−B(2), B(1)−B(3), and B(1)−B(5). (See Figure 2 for atom numbering.) This was done by taking an average of these three (p_1) and defining two differences: B(1)−B(3) − B(1)−B(2) (p_2) and B(1)−B(3) − B(1)−B(5) (p_3). On the basis of geometry optimization calculations, all C−H bonds were assumed to be the same length, as were the set of terminal B−H bonds and the remaining group of bridging B−H bonds. The bonds to hydrogen were thus defined in a way similar to that of the B−B bonds, first taking the average of the three groups (p_8) and then defining two differences, B−H$_b$ − C−H (p_9) and B−H$_b$ − B−H$_t$ (p_{10}), where subscript b stands for bridging and t for terminal. The carbon atoms were placed on the *xy* plane (one of the planes of symmetry) and were positioned using a distance from the origin (p_5) and an angle from the *x* axis (p_6). For the purposes of this model, the *x* axis was defined as that axis lying perpendicular to the B(1)−B(3) bond in the direction of the nonbonded distance C(6)···C(9); the *y* axis forms the axis of rotation, and the *z* axis lies along the B(1)−B(3) bond. The origin was defined as being the midpoint between atoms B(1) and B(3).

Six bond angles were also included as independent parameters, of which B(5)−B(1)−B(3) (p_7) was the only one exclusively involving heavy atoms. The remaining bond angles (p_{11}−p_{15}) were required for positioning the hydrogen atoms, as shown in Table 2. Three torsional angles were used, B(4)−B(3)−B(1)−B(5) (p_{16}) being the only one relating only heavy atoms. The torsions B(3)−B(1)−B(5)−H(15) and B(8)−B(5)−B(10)−H(23) (p_{17} and p_{18}) were used to position hydrogen atoms H(15) and H(23), respectively. The remaining parameter (p_4) was used to position atoms B(2) and B(4) and was defined as the angle made by B(4), the origin, and the *x* axis.

Results and Discussion

GED Structure Refinement. The GED refinements were performed using the SARACEN method,[37] incorporating flexible restraints. A Cartesian force field was obtained from the RHF/6-31G* calculation and converted into a force field described by a set of symmetry coordinates using the program SHRINK.[38] From this, the root-mean-squared amplitudes of vibration (u_{h1}) and perpendicular distance corrections (k_{h1}) were generated.

All 18 independent parameters were refined; 11 of them were restrained to the MP2/6-31G* calculated values, as shown in Table 2. Four dependent parameters (d_1−d_4) were also restrained to their MP2/6-31G* values during the refinement. These were defined as the differences between the B(5)−C(6) and B(2)−C(6) bonds (d_1), B(2)−B(5) −

---

(34) Fleischer, H.; Wann, D. A.; Hinchley, S. L.; Borisenko, K. B.; Lewis, J. R.; Mawhorter, R. J.; Robertson, H. E.; Rankin, D. W. H. *Dalton Trans.* **2005**, 3221.

(35) Hinchley, S. L.; Robertson, H. E.; Borisenko, K. B.; Turner, A. R.; Johnston, B. F.; Rankin, D. W. H.; Ahmadian, M.; Jones, J. N.; Cowley, A. H. *Dalton Trans.* **2004**, 2469.

(36) Ross, A. W.; Fink, M.; Hilderbrandt, R. *International Tables for Crystallography*; Wilson, A. J. C., Ed.; Kluwer Academic Publishers: Dordrecht, The Netherlands, 1992; Vol. C, p 245.

(37) a) Mitzel, N. W.; Smart, B. A.; Blake, A. J.; Robertson, H. E.; Rankin D. W. H. *J. Phys. Chem.* **1996**, *100*, 9339. (b) Blake, A. J.; Brain, P. T.; McNab, H.; Miller, J.; Morrison, C. A.; Parsons, S.; Rankin, D. W. H.; Robertson, H. E.; Smart, B. A. *J. Phys. Chem.* **1996**, *100*, 12280. (c) Mitzel, N. W.; Rankin, D. W. H. *Dalton Trans.* **2003**, 3650.

(38) Sipachev, V. A. *J. Mol. Struct.* (*THEOCHEM*) **1985**, *121*, 143.

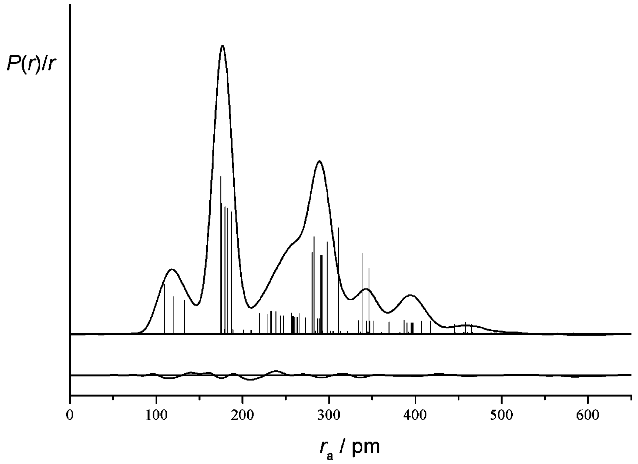

Figure 5. Experimental and difference (experimental − theoretical) radial-distribution curves, $P(r)/r$, for **2**. Before Fourier inversion, the data were multiplied by s; $\exp[(-0.00002s^2)/(Z_C - f_C)(Z_B - f_B)]$.

B(5)−C(6) (d_2), B(1)−B(2) − B(5)−C(6) (d_3), and B(5)−B(10) − B(2)−B(5) (d_4). In addition, seven groups of vibrational amplitudes were refined (see the Supporting Information, Table S2). Two of these groups (amplitudes corresponding to heavy atom distances from 160 to 200 pm and 280 to 320 pm) refined unrestrained, whereas each of the remaining five groups of amplitudes was restrained with an uncertainty of ca. 10% of its calculated (RHF/6-31G*) value.

The final refinement produced an R factor (R_G) of 0.057 ($R_D = 0.036$). The quality of fit can also be assessed in terms of the radial-distribution curve (Figure 5) and molecular-scattering intensity curves (see the Supporting information, Figure S1), showing good agreement between the model and experimental data. The least-squares correlation matrix is included in the Supporting Information (Table S3).

ab Initio and GIAO Calculations. The molecular structures of **2**−**4** were proposed on the basis of their ^{11}B NMR data, which are fully compatible with C_{2v} symmetry (three 2:4:2 doublets). Molecules **2**−**4** possess open six-membered faces, which assume boat conformations in accord with the qualitative connectivity considerations of Williams.[39] van der Waals' radii of the heteroatoms in these contiguous cluster monoheteroatomic boranes, i.e., in those that have more than one electron-rich heteroatom center in the cluster, dictate the flattening of the open hexagonal face, NB_2NB_2 being the most flattened one. A measure of this flattening is provided by the X−B(5)···B(7)−B(8) dihedral angle and is also reflected in the E−B nearest-neighbor separations as well as in the B(5)−E−B(7) triangles. These internal coordinates are presented in Table 3. Table 3 also summarizes other RMP2(fc) distances and angles and provides comparison with electron-diffraction parameters restrained by theoretical calculations in the case of **2**. In general, there is no discrepancy between these two structural characterizations of the dicarbaborane. This finding is corroborated by a single-point energy calculation for the experimental geometry of **2** at the MP2/6-31G* level, which finds this structure only 5.6 kJ mol^{-1} above the fully optimized one, suggesting that the corresponding GED parameters describe the gas-phase molecular geometry well. The geometries of **2**−**4** optimized at the MP2/6-31G* and MP2/962(d) levels are depicted in Figures 2−4, respectively.

Table 3. Selected Geometrical Parameters for **2**−**4**[a] (for $X_2B_8H_n$)

	X = C, n = 14 ($C_2B_8H_{14}$)		X = N, n = 12 ($N_2B_8H_{12}$)	X = Se, n = 10 ($Se_2B_8H_{10}$)
	GED	MP2/6-31G*		
X−B(2)	167.0(5)	166.0	155.3	207.1
X−B(5)	175.1(2)	173.8	153.7	209.1
B(1)−B(2)	175.2(2)	174.0	176.1	175.9
B(2)−B(5)	178.5(3)	176.8	191.4	189.2
B(1)−B(3)	182.1(3)	181.0	180.6	178.1
B(1)−B(5)	180.1(3)	179.1	181.6	178.7
B(7)−B(8)	188.0(4)	186.4	180.0	182.5
B−H_t mean	120.1(3)	118.9	119.1	118.9
X−H mean	110.2(6)	108.8	101.6	
B−H_b	132.8(5)	131.4	132.6	131.5
B(5)−X−B(7)	112.8(4)	111.9	120.0	92.9
X−B(5)···B(7)−B(8)	129.9(7)	131.3	156.7	134.5

[a] Distances in picometers, angles in degrees.

The good agreement between the experimental and calculated ^{11}B NMR chemical shifts, in particular at the GIAO-MP2 level (see Table 1), strongly suggests that the RMP2(fc)/6-31G* and RMP2(fc)/962(d) internal coordinates are good representations of the molecular geometries of **2**−**4** in solution.

Whereas the NMR results for B(1,3) show no large dependence on the theoretical level, those for the other two resonances (B(2,4) and B(5,7,8,10)) are very sensitive to the inclusion of electron correlation. (Compare HF and MP2 values in Table 1.) Large deviations can occur at the HF level (up to 7 ppm for **2** and **4**) that are significantly reduced at GIAO-MP2 (maximum deviation = 2.1 ppm for B(2,4) in **4**). The performance of this method for **2**−**4** is similar to that for strained and unstrained carbaboranes.[40]

For the Se species, **4**, the good performance of the GIAO-MP2 method could be fortuitous, if shortcomings of this approach (and those of basis-set deficiencies) compensate for other errors stemming from the neglect of relativistic effects. The effect of a heavy atom on the chemical shift of a light atom to which it is bonded can be extreme when elements from the fourth row and beyond are present, but can also be noticeable for third-row elements. For example, spin−orbit (SO) effects of up to 17 ppm have been computed for $\delta(^{13}C)$ in CH_3Br.[41] The development of quantum-chemical methods that incorporate relativistic effects in chemical-shift calculations is an active area of research.[42] We have assessed scalar and spin−orbit relativistic effects on the theoretical ^{11}B chemical shifts by using a suitable ECP and by performing an explicit ZORA-SO computation, respectively. The scalar effects have been probed by comparing GIAO-HF/962+(d) and GIAO-HF/ECP+(d) results, which are

---

(39) Williams, R. E. *Adv. Inorg. Chem. Radiochem.* **1976**, *18*, 95.

(40) Bühl, M.; Gauss, J.; Hofmann, M.; Schleyer, P. v. R. *J. Am. Chem. Soc.* **1993**, *115*, 12385.

(41) Malkin, V. G.; Malkina, O. L.; Salahub, D. *Chem. Phys. Lett.* **1996**, *261*, 335.

(42) Kaupp, M., Bühl, M., Malkin V. G., Eds.; *Calculation of NMR and EPR Parameters: Theory and Applications.* Wiley-VCH: Weinheim, Germany, 2004.

found to differ by less than 1 ppm for any of the ^{11}B nuclei. The SO contributions are also found to be small, not exceeding 0.5 ppm in the ZORA-SO approach.

That the SO effects on $\delta(^{11}B)$ are so small (much smaller than the corresponding effects on ^{13}C chemical shifts in bromoalkanes[41]), can be rationalized by the bonding in the heteroborane cluster. SO effects are transmitted via a Fermi-contact type relay mechanism, which is very effective when bonds with high s character are involved.[43] However, according to natural bond orbital analysis,[5] the bonding between Se and B atoms in **4** has predominantly p character, e.g., $sp^{5.36}$ for Se(6)−B(2), i.e., 84.1% p character [RMP2-(fc)/641(d)]. Consequently, no large SO corrections are to be expected for calculations of the ^{11}B magnetic shieldings in **4** or, presumably, in other polyhedral selenaboranes as well.[44]

Although ^{77}Se NMR spectroscopy is a convenient and versatile method for characterizing selenium compounds,[45] ^{77}Se NMR data for polyhedral boranes are extremely rare. To the best of our knowledge, the only example to have been reported, apart from some selenaborole derivatives,[45,46] is $[H_3B\text{-}\mu^2\text{-}Se(B_2H_5)]^-$, for which $\delta(^{77}Se) = -473.8$.[47] A ^{77}Se chemical shift in a similar region is predicted for **4** [$\delta = -122$ for the GIAO-MP2/962+(d)//MP2/962(d) level; for HF, $\delta = -282$], and we note this value for future reference. With very similar levels of theory, ^{77}Se chemical shifts for a larger set of inorganic and organic selenium compounds have been reproduced to an accuracy of better than 100 ppm over a total chemical shift range of ca. 2800 ppm.[48]

In summary, we have characterized the molecular structures of three heterodecaboranes derived from [*arachno*-$B_{10}H_{14}]^{2-}$ at appropriate levels of ab initio MO theory. The accuracy of the optimized geometric parameters has been confirmed by the excellent agreement of the ^{11}B chemical shifts calculated at the GIAO-MP2 level with the experimental values. The credibility of the GED-derived structure of **2** has been ascertained by the same method. For these heteroborane clusters, electron correlation effects on the computed $\delta(^{11}B)$ values are quite substantial, and it is necessary to go beyond the HF level in the NMR computation. The GIAO-MP2 approach presents itself as method of choice for these systems. Further methodological developments to reduce the computational effort in these demanding calculations[49] would be desirable in order to open the way for applications to larger heteroborane derivatives. Meanwhile, the GIAO-B3LYP is an acceptable alternative, although it should always be remembered that there are structures for which the B3LYP method gives poor results, particularly when second-row atoms are present.

Acknowledgment. We thank the Ministry of Education of the Czech Republic for financial support (Project LC523). S.A.H. thanks the School of Chemistry at the University of Edinburgh for jointly funding a studentship with the EPSRC, which also funded the electron-diffraction research (Grant GR/R17768) and currently funds D.A.W. and H.E.R. (Grant EP/CS13649).

Supporting Information Available: Listings of GED data analysis parameters, selected distances, amplitudes of vibration and perpendicular amplitude correction coefficients derived from or used in the GED refinement, the least-squares correlation matrix for the GED refinement, atomic coordinates for each structure, and GED molecular scattering intensity curves (pdf). This material is available free of charge via the Internet at http://pubs.acs.org.

IC060296V

---

(43) Kaupp, M.; Malkina, O. L.; Malkin, V. G. Pyykkö, P. *Eur. J. Chem.* **1998**, *4*, 118.

(44) If large SO contributions were to arise from FC interactions, substantial ^1J(Se, B) spin−spin coupling constants would be expected as well (cf. ref 43); however, such couplings are usually very small or cannot be resolved at all (cf. ref 46). For selenaboroles, very small ^1J(Se, B) values below ca. 10−20 Hz have been estimated: Fussstetter, H.; Nöth, H.; Wrackmeyer, B.; McFarlane, W. *Chem. Ber.* **1977**, *110*, 3172. Köster, R.; Seidel, G.; Boese, R.; Wrackmeyer, B. *Chem. Ber.* **1988**, *121*, 1955.

(45) Duddek, H. *Prog. NMR Spectrosc.* **1995**, *27*, 1.

(46) Köster, R.; Seidel, G.; Boese, R.; Wrackmeyer, B. *Chem. Ber.* **1988**, *121*, 1955.

(47) Binder, H.; Duttlinger, I.; Loos, H.; Locke, K.; Pfitzner, A.; Flad, J.-J.; Savin, A.; Kohout, M. *Z. Anorg. Allg. Chem.* **1995**, *621*, 400.

(48) See, for example, ref 26b. For a DFT study, see Schreckenbach, G.; Ruiz-Morales, Y.; Ziegler, T. *J. Chem. Phys.* **1996**, *104*, 8605.

(49) Gauss, J.; Werner, H. *Phys. Chem. Chem. Phys.* **2000**, *2*, 2083.